
Ensemble sampler for infinite-dimensional inverse problems

Jeremie Coullon · Robert J. Webber

Abstract We introduce a new Markov chain Monte Carlo sampler for infinite-dimensional Bayesian inverse problems. The new sampler is based on the affine invariant ensemble sampler, which we extend for the first time to function spaces. The new sampler is more efficient than preconditioned Crank-Nicolson, yet it requires no gradient information or posterior covariance information, making the sampler broadly applicable.

Keywords Bayesian inverse problems · Markov chain Monte Carlo · infinite-dimensional inverse problems · dimensionality reduction

Mathematics Subject Classification (2010) 65C05 · 35R30 · 62F15

1 Introduction

In many Bayesian inverse problems, Markov chain Monte Carlo (MCMC) methods are needed to approximate distributions on infinite-dimensional function spaces, for example, in groundwater flow [12], medical imaging [9], and traffic flow [6]. Yet designing efficient and broadly applicable MCMC methods for function spaces has proved challenging.

The earliest proposed functional sampler was preconditioned Crank-Nicolson (PCN, [4]). PCN is easy to code and broadly applicable. However, when parameters are correlated or multimodal under the Bayesian posterior distribution, PCN requires a large number of

iterations to accurately calculate statistics [5]. In contrast, newly developed gradient-based [5,8,2] or preconditioned [18,15] MCMC methods sample more efficiently, but the new samplers require gradient or covariance information, which can be challenging to obtain.

This raises the question: are there functional samplers that outperform PCN without requiring any gradient or covariance information? A gradient-free sampler is needed when the forward model has a legacy code base and obtaining derivatives is difficult or impossible. A covariance-free sampler is needed when estimating the posterior covariance matrix would require excessive computational resources.

In the literature on finite-dimensional MCMC, there is a gradient-free sampler that avoids explicit covariance estimation yet adapts naturally to the covariance structure of the sampled distribution. This sampler, called the affine invariant ensemble sampler (AIES, [11]), is easy to tune, easy to parallelize, and efficient at sampling spaces of moderate dimensionality ($d \leq 20$). AIES is used extensively due to its implementation in the popular `emcee` package for python [10].

The main contribution of this work is to propose the functional ensemble sampler (FES), which combines AIES and PCN. The first step of the new sampler is to calculate the Karhunen–Loève (KL) expansion for a Gaussian prior distribution. Then, FES samples the posterior distribution on the leading KL coefficients using AIES and samples the complementary subspace using PCN. By combining AIES and PCN, we obtain a functional sampler that is stable, efficient, and applicable across a large range of Bayesian inverse problems.

In two numerical examples, we test FES on challenging inverse problems with a functional parameter and one or more scalar parameters. In our first example, we

Jeremie Coullon
Lancaster University, LA1 4YF United Kingdom
E-mail: j.coullon@lancaster.ac.uk

Robert J. Webber
New York University, 10012 New York, United States
E-mail: rw2515@nyu.edu

apply Bayesian inversion to the advection equation

$$\begin{cases} \frac{\partial \rho}{\partial t} + c \frac{\partial \rho}{\partial x} = 0, & t > 0, \\ \rho = \rho_0, & t = 0. \end{cases} \quad (1)$$

We simultaneously estimate the advection speed $c \in \mathbb{R}$ and the initial condition ρ_0 from a set of noisy observations. We find that PCN mixes slowly because c and ρ_0 are highly correlated under the posterior distribution. However, FES mixes more quickly, reducing integrated autocorrelation times [16] by two orders of magnitude.

In our second example, we apply Bayesian inversion to the Langevin diffusion

$$\begin{cases} dX = P dt, & t > 0, \\ dP = -\alpha X dt + \sigma dW, & t > 0, \\ X = P = 0, & t = 0. \end{cases} \quad (2)$$

We simultaneously estimate the drift parameter α , the diffusion parameter σ , and the posterior path X_t from noisy observations. We find that PCN is inefficient for this problem because α is multimodal under the posterior distribution. However, FES efficiently traverses the modes, leading to faster sampling compared to PCN and compared to an alternative sampler that explicitly estimates a posterior covariance matrix.

The rest of the paper is organized as follows. Section 2 reviews the PCN and AIES samplers. Section 3 introduces the new ensemble sampler for function spaces. Section 4 presents numerical examples. Lastly, section 5 concludes. Code to reproduce the examples is available on Github¹.

2 Background on MCMC samplers

2.1 Preconditioned Crank-Nicolson

In this section, we explain why it is difficult to approximate the Bayesian posterior distribution on an infinite-dimensional function space and we review the preconditioned Crank-Nicolson sampler (PCN, [4]) which can be used for this approximation task.

In an infinite-dimensional Bayesian inverse problem, a typical goal is estimating a posterior distribution

$$\pi(du) \propto \exp(\phi(u)) \pi_0(du), \quad (3)$$

where u is a square-integrable function on a bounded domain $U \subseteq \mathbb{R}^d$, $\phi(u)$ is a log-likelihood functional, and $\pi_0 = \mathcal{N}(0, C)$ is a Gaussian prior distribution.

To estimate π , we must first select a finite-dimensional approximation space and then use MCMC to sample

π restricted to this space. However, this MCMC-based approach can be difficult. A high-dimensional approximation space is needed to accurately calculate statistics of the posterior distribution. But as we increase the dimensionality, the acceptance probability for a standard MCMC sampler, such as the Metropolis random walk sampler [13], sinks to zero. Hence, the MCMC sampler takes an increasingly long time to move anywhere, and sampling from π becomes a practical impossibility [5].

PCN solves the problem of vanishing acceptance probabilities by proposing MCMC moves that are *always* accepted under the prior. Because of this stability property, even as we increase the dimensionality of the approximation space, the average acceptance probability remains bounded away from zero in PCN.

Starting from a position U , the PCN update is

$$\tilde{U} = \sqrt{1 - \omega^2} U + \omega \xi, \quad (4)$$

where $\xi \sim \mathcal{N}(0, C)$ is a random draw from the Gaussian prior and $\omega \in (0, 1]$ is a step size parameter. If $\omega \approx 0$, the proposal is a small perturbation of U , whereas if $\omega = 1$ the proposal is independent from U . The main computational cost of PCN comes from evaluating the acceptance probability

$$\min \left\{ 1, \exp \left(\phi(\tilde{U}) - \phi(U) \right) \right\}, \quad (5)$$

which requires calculating the log-likelihood functional at the proposed parameter value \tilde{U} .

In summary, PCN is a simple, widely applicable approach that requires little more than making cheap proposals and evaluating the log-likelihood at the proposed parameter values. The main limitation of PCN, however, is the slow sampling speed for poorly scaled or multimodal posterior distributions (e.g., [15, 18]).

2.2 Affine invariant ensemble sampler

The affine invariant ensemble sampler (AIES, [11]) is a finite-dimensional MCMC sampler with the remarkable property of *affine invariance*. Affine invariance means that the sampler remains completely unchanged if the state space is stretched, compressed, or translated by an affine transformation $x \mapsto Ax + b$. Because of this property, AIES efficiently samples from distributions that are wide in some directions and narrow in other directions. These ‘‘poorly scaled’’ distributions would cause problems for other samplers, but they do not compromise the performance of AIES.

AIES uses an ensemble of walkers $\vec{X} = (X_1, \dots, X_L)$ to sample from a product density $\pi(x_1) \cdots \pi(x_L)$, with each walker taking values in \mathbb{R}^M . To update the ensemble, AIES proposes to slide one walker toward or away

¹ https://github.com/jeremiecoullon/functional_ensemble_sampler

from another walker. Then, AIES accepts or rejects the proposal according to a Metropolis-Hastings acceptance probability. Since the proposals and acceptance probabilities are invariant under affine transformations, the scheme is affine invariant overall.

To perform the AIES proposal step, we choose a walker X_i and a second walker $X_j \neq X_i$. Then, we propose moving the walker X_i to the new position

$$\tilde{X}_i = X_i + (1 - Z)(X_j - X_i), \quad (6)$$

where $Z \in [1/a, a]$ is a random number with density $g(Z) \propto 1/\sqrt{z}$, and a is a step size parameter that is typically set to $a = 2$. The main computational cost of AIES comes from evaluating the acceptance probability

$$\min \left\{ 1, Z^{M-1} \frac{\pi(\tilde{X}_i)}{\pi(X_i)} \right\}. \quad (7)$$

AIES is an efficient sampler for low- and moderate-dimensional problems ($M \leq 20$). Additionally, in high-dimensional problems, there is often a low-dimensional subspace that requires the most careful sampling. In the sections to follow, we describe how AIES can be used on this low-dimensional subspace, thereby improving the sampling for infinite-dimensional inverse problems.

Remark 1 A parallel implementation of AIES is available in the `emcee` package for python [10]. In this version of AIES, we modify the dynamics by splitting the walkers into two groups and sampling in two stages. Initially, we select walkers from the first group and slide these walkers toward or away from walkers in the second group. Then, we select walkers from the second group and slide these walkers toward or away from walkers in the first group. By using this modified dynamics, we can conduct AIES in parallel across multiple processors, helping to spread out the computational cost.

3 New ensemble sampler

In this section, we introduce the Karhunen-Loève (KL) expansion, which is a central component of our new functional ensemble sampler. After introducing the KL expansion, we provide pseudocode for the new sampler and explain its advantages over alternative methods.

3.1 KL expansion

The KL expansion [17] is a rapidly converging basis expansion for functions drawn from a Gaussian distribution $\mathcal{N}(0, C)$. The KL expansion decomposes a function into a linear combination of “KL modes” η_1, η_2, \dots ,

which are eigenfunctions of a trace-class covariance operator C . For a random function $\xi \sim \mathcal{N}(0, C)$, the KL expansion takes the form

$$\xi = \sum_{i=1}^{\infty} \langle \eta_i, \xi \rangle \eta_i, \quad (8)$$

where $\langle \cdot, \cdot \rangle$ denotes the inner product in L^2 . The KL coordinates $\langle \eta_i, \xi \rangle$ are independent Gaussian random variables with variances $\lambda_1 \geq \lambda_2 \geq \dots$ given by the eigenvalues of C .

The KL expansion converges as rapidly as possible, in the sense of minimizing the mean squared error

$$\mathbb{E}_{\xi \sim \mathcal{N}(0, C)} \left\| \xi - \sum_{i=1}^L \langle \eta_i, \xi \rangle \eta_i \right\|_{L^2}^2, \quad (9)$$

for any $L \geq 1$. Because the KL expansion converges so rapidly, the first few coordinates explain most of the variance in ξ , and the complementary subspace explains much less of the variance. For example, when ξ is a Brownian motion on $[0, 1]$, the eigenvalues of the covariance operator are $\lambda_i = (i - \frac{1}{2})^{-2} \pi^{-2}$ for $i \geq 1$. Hence, the first five KL coordinates account for 96% of the variance in ξ ; the complementary subspace accounts for just 4% of the variance.

We now consider the implications of the KL expansion for Bayesian inference. We can decompose any functional parameter U in terms of the KL modes

$$U = \sum_{i=1}^{\infty} U_i \eta_i, \quad U_i = \langle \eta_i, U \rangle. \quad (10)$$

Under the prior distribution $\pi_0 = \mathcal{N}(0, C)$, the U_i coordinates are independent Gaussians, whose variance decreases rapidly as $i \rightarrow \infty$. In contrast, under the posterior distribution $\pi(du) \propto \exp(\phi(u)) \pi_0(du)$, the U_i coordinates have an unknown distribution that must be approximated through sampling.

While the U_i coordinates are unknown under the posterior, the prior distribution restricts the values that these coordinates can take. The restrictions on the high U_i coordinates are especially strong. Since these coordinates are tightly concentrated Gaussians under the prior, they are constrained to be nearly Gaussian under the posterior also. In contrast, the leading KL coordinates are less constrained. The posterior distribution on these coordinates can be stretched, pinched, or otherwise distorted compared to the prior.

As a consequence, the KL coordinates divide the Bayesian MCMC sampling into an easy part and a hard part. Sampling the high KL coordinates is the easy part. Since the posterior distribution is nearly the same as the prior distribution, PCN samples these coordinates

efficiently. In contrast, sampling the leading KL coordinates is much harder and PCN may fail to provide the needed efficiency.

3.2 Functional ensemble sampler

To improve MCMC sampling for infinite-dimensional inverse problems, we propose a Metropolis-within-Gibbs sampler that alternates between using AIES to sample the leading KL coordinates and using PCN to sample the complementary subspace. We call this approach the functional ensemble sampler (FES) and provide pseudocode for the method below.

Algorithm 1 (Functional ensemble sampler)

To sample a distribution $\pi(du) \propto \exp(\phi(u)) \pi_0(du)$ with $\pi_0 = \mathcal{N}(0, C)$, perform the following steps:

1. Identify a matrix J whose columns are the first M eigenvectors of C . Set $P = JJ^T$ and $Q = I - JJ^T$.
2. Initialize an ensemble of walkers (X_1^0, \dots, X_L^0) .
3. For $\tau = 0, 1, \dots$:

(a) For $i = 1, \dots, L$:

- i. Randomly choose a walker $X_j^{2\tau} \neq X_i^{2\tau}$.
- ii. Propose the update

$$\tilde{X}_i^{2\tau} = X_i^{2\tau} + (1 - Z)P(X_j^{2\tau} - X_i^{2\tau}), \quad (11)$$

where $Z \in [1/a, a]$ has density $g(z) \propto 1/\sqrt{z}$.

iii. Set $X_i^{2\tau} = \tilde{X}_i^{2\tau}$ with probability

$$\min \left\{ 1, Z^{M-1} \frac{\pi(\tilde{X}_i^{2\tau})}{\pi(X_i^{2\tau})} \right\}. \quad (12)$$

(b) Set $(X_0^{2\tau+1}, \dots, X_L^{2\tau+1}) = (X_0^{2\tau}, \dots, X_L^{2\tau})$.

(c) For $i = 1, \dots, L$:

i. Propose the update

$$\tilde{X}_i^{2\tau+1} = PX_i^{2\tau+1} + Q \left(\sqrt{1 - \omega^2} X_i^{2\tau+1} + \omega \xi \right), \quad (13)$$

where $\xi \sim \mathcal{N}(0, C)$.

ii. Set $X_i^{2\tau+1} = \tilde{X}_i^{2\tau+1}$ with probability

$$\min \left\{ 1, \exp \left(\phi(\tilde{X}_i) - \phi(X_i) \right) \right\}. \quad (14)$$

(d) Set $(X_0^{2\tau+2}, \dots, X_L^{2\tau+2}) = (X_0^{2\tau+1}, \dots, X_L^{2\tau+1})$.

The main tuning parameter in FES is the number M , which controls how many KL coordinates are included in the AIES sampling. When $M = 0$, no AIES sampling is performed, so the algorithm reduces to PCN. As M increases, FES begins to outperform PCN. However, if M increases past 20, the performance deteriorates, since AIES is only an efficient sampler for subspaces of dimension 20 and lower. To our knowledge, FES is the first sampler that outperforms PCN without requiring gradients or a posterior covariance matrix.

3.3 Limitations, extensions, and comparisons

To explain the limitations of FES, we introduce the idea of a *likelihood-informed subspace* (LIS, [8]). An LIS is a low-dimensional linear subspace with substantially different prior and posterior marginal distributions. Moreover, conditioning on an LIS ensures that the differences between prior and posterior distributions become small. The idea of an LIS is important because enhanced sampling is needed on an LIS, but PCN is an efficient sampler in the directions orthogonal to the LIS [8, 7, 3].

The functional ensemble sampler relies on the assumption that the leading 10 or 20 KL coordinates contain a LIS, an assumption ensuring that PCN can efficiently sample the complementary subspace. This assumption is often but not always satisfied in practice. By considering a sufficiently large number of KL coordinates, we can always find an LIS. However, the required number of coordinates may be much larger than 20. For example, a large number of KL coordinates is needed if the posterior distribution emphasizes solutions that are not very smooth, which can happen if the observational noise in the problem is small. When the required number of KL coordinates is higher than 20, FES may no longer provide an efficient sampling solution, although it is still not slower than PCN. It is an open problem to design an efficient gradient-free, covariance-free sampler for such problems.

The number of KL coordinates to use in FES is a tuning decision, with the optimal number changing depending on the estimation problem. It is tempting to choose the number of coordinates based solely on the prior covariance structure, so that the KL coordinates explain at least 90% or 95% of the prior variance. However, while simple and easy to implement, we find this strategy not to be robust. Rather, a helpful approach for tuning FES is to adjust the number of KL coordinates as necessary during the sampling, making sure the PCN sampler can take large steps ($\omega \geq 0.5$) with acceptance rate $\geq 20\%$. We recommend the parameter range $5 \leq M \leq 10$ as a default.

Ideally, we would extend FES by applying AIES directly to a likelihood-informed subspace while applying PCN to the complementary subspace. This would eliminate the reliance on the Karhunen-Loève (KL) expansion and improve computational efficiency. However, to our knowledge, all the available methods for identifying an LIS involve calculating gradients (e.g., [7]) or calculating posterior covariance matrices (e.g., [3]). Developing broadly applicable tools for identifying an LIS remains a challenge for future research.

Other extensions to FES are also possible. Whereas Algorithm 1 presents a sequential implementation of

FES, there is also a parallel implementation, which incorporates the modified AIES sampling discussed in Remark 1. Parallelization is useful for spreading out the computational cost of likelihood evaluations across multiple processors, thereby speeding up the sampling.

Another extension of FES involves jointly sampling functional and scalar parameters in a Bayesian inverse problem. It is simple to include the scalar parameters as additional dimensions in the AIES subspace. We regard this extension of FES as especially useful and present examples involving both functional and scalar parameters in Section 4.

Lastly, we mention an alternative MCMC method for infinite-dimensional inverse problems that shares features with FES. Similar to FES, the hybrid sampler [18] is a gradient-free approach that uses PCN to sample high KL coordinates. However, to sample the leading KL coordinates, the method uses Gaussian random walk perturbations, where the covariance of the perturbations is determined from the estimated posterior covariance matrix. In our experiments, we find that the hybrid sampler is very efficient when the posterior distribution is nearly Gaussian and the posterior covariance matrix is accurately estimated (even slightly more efficient than FES). However, limitations of the hybrid sampler include sensitivity to non-Gaussian posterior distributions and long adaptation periods that are required for covariance estimation. Adaptively estimating all the entries in a posterior covariance matrix is known to be a slow process, potentially requiring $\mathcal{O}(10^6)$ decorrelation timescales [14], and we present additional evidence of this slow convergence in section 4.2. For short sampling runs, the covariance estimates are not accurate and the hybrid sampler offers little improvement over PCN. In contrast, FES is a fast sampler for many non-Gaussian distributions (see Section 4.2) and requires no adaptation period, making the method suitable for short sampling runs.

4 Numerical examples

In this section, we present examples of FES applied to Bayesian inverse problems with both functional and scalar parameters. The first example, the advection equation, tests FES's efficiency when sampling correlated parameters. The second example, path reconstruction for Langevin dynamics, tests FES's efficiency when sampling a mildly multimodal distribution.

In both examples, we fix the AIES step size to $a = 2$, as recommended in [10], and we tune the PCN step size ω to give an acceptance rate of 20%. To ensure robust statistics, we remove the first 10% of each trajectory as

burn-in, and we run the trajectories at least 100 times as long as the integrated autocorrelation time [16].

4.1 Advection equation

We consider the advection equation $\frac{\partial \rho}{\partial t} + c \frac{\partial \rho}{\partial x} = 0$, a simple first-order equation that is a prototype for more general hyperbolic PDEs. The advection equation's solution is characterized by an initial condition $\rho_0(x)$ and a wave speed $c \in \mathbb{R}$. The equation transports the initial condition to the left or right with speed given by c . The solution at (x, t) can therefore be explicitly written as

$$\rho(x, t) = \rho_0(x - ct). \quad (15)$$

Through Bayesian inversion, we can recover the initial condition and wave speed from noisy observation of flow at detectors in the xt -plane. Flow can be calculated from density and speed and is given by the relation $q = \rho c$. When flow is the only quantity observed, the initial condition and wave speed become highly correlated in the posterior distribution, which makes MCMC sampling difficult.

In our Bayesian model, we set a uniform prior on the wave speed $c \sim \mathcal{U}(0, 1.4)$, which restricts the direction of the flow. We set a Gaussian prior on the initial condition ρ_0 with a mean of 100 and a covariance function given by

$$k(x, x') = 130 \exp\left(-\frac{1}{2}(x - x')^2\right). \quad (16)$$

We observe the flow $q = \rho c$ at locations $x = 2, 6, 10$ and times $t = 1, 1.5, 2$, subject to independent $\mathcal{N}(0, 0.04)$ observational noise. We generate a true solution by setting $c_{true} = 0.5$ and randomly draw an initial condition and observational noise according to the Bayesian model. Lastly, we discretize ρ_0 using 200 gridpoints, equally spaced between $x = 0$ and $x = 10$.

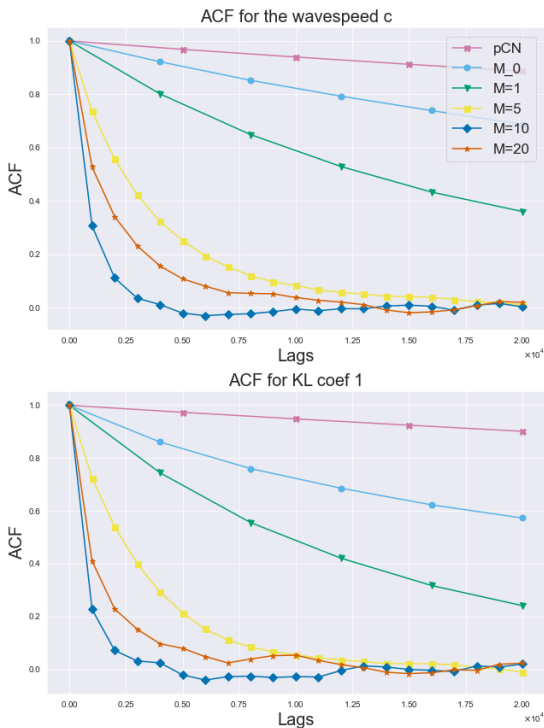
We apply FES to infer the parameters c and ρ_0 from the noisy observations using $L = 100$ walkers. To study the dependence of FES on parameters, we consider varying the size of the AIES subspace. In all trials, the AIES subspace includes the wave speed parameter c . Additionally, the subspace includes either $M = 0, 1, 5, 10, 20$ KL coordinates. For comparison, we also run a standard PCN-based sampler that simultaneously proposes PCN updates for ρ_0 and Gaussian random walk updates for c with variance $\sigma^2 = 5 \times 10^{-5}$.

Table 1 reports the PCN step size for the different samplers. As the parameter M increases, we find that we can take larger PCN steps while maintaining a 20% acceptance rate. These large step sizes indicate efficient sampling of the complementary subspace.

PCN step size						
	PCN	$M=0$	$M=1$	$M=5$	$M=10$	$M=20$
ω	0.01	0.04	0.05	0.15	0.60	1.00

Table 1: Step size ω for different samplers.

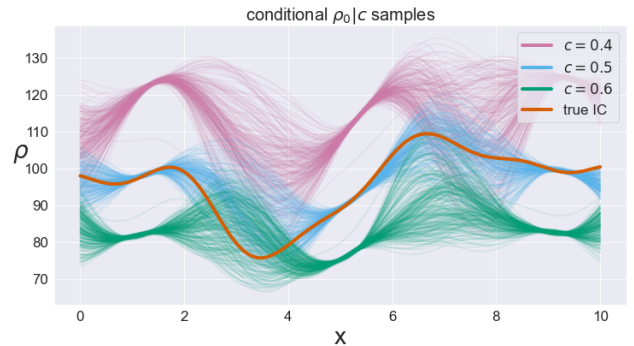
To gauge the performance of the different samplers, we calculate the autocorrelation function (ACF) and integrated autocorrelation time (IAT) for various observables. We show the ACFs in Figure 1 and IATs in Table 2. The results demonstrate that choosing $M = 10$ leads to the most efficient sampling. Moreover, when $M = 10$, FES improves computational efficiency by two orders of magnitude compared to PCN.

Fig. 1: ACF curves for wave speed c and the first KL coefficient.

Integrated autocorrelation time \div 1000						
	PCN	$M=0$	$M=1$	$M=5$	$M=10$	$M=20$
c	360	130	50	7.7	1.5	4.3
ϕ_1	390	110	30	6.8	1.4	3.1
ϕ_5	290	46	55	11	1.1	1.9
ϕ_{15}	280	30	16	12	1.0	1.2
ϕ_{100}	310	43	20	11	1.1	1.4

Table 2: IATs for c and several KL coefficients with the fastest IATs in bold. All IATs have been divided by 1000 to improve readability.

Figure 2 shows posterior samples of ρ_0 conditioned on several values of c . As the wave speed c decreases, the initial density rises and shifts slightly to the right. This relationship demonstrates a strong dependence between the wave speed c and the first few KL coefficients. Moreover, the high correlations between parameters explain the dramatic benefits of using FES for this problem. By isolating correlated parameters within a low-dimensional subspace and sampling the correlated variables efficiently, FES eliminates the major bottlenecks in the sampling.

Fig. 2: Samples of the initial condition ρ_0 conditioned three values of the wave speed c .

4.2 Path reconstruction for Langevin dynamics

In this example, we consider the oscillatory Langevin dynamics where position X_t and momentum P_t evolve according to the stochastic differential equation (SDE)

$$\begin{cases} dX = P dt, & t > 0, \\ dP = -\alpha X dt + \sigma dW, & t > 0, \\ X = P = 0, & t = 0. \end{cases} \quad (17)$$

Based on noisy observations of position, we aim to estimate the parameters α and σ , as well as the posterior path X_t . To obtain the posterior path, we must first infer the driving Brownian motion W_t and the two scalar parameters. Then, we recover the posterior path by solving the SDE.

In our Bayesian model, we use the following priors:

$$\alpha \sim \text{Exp}(12), \quad \sigma \sim \text{Exp}(4), \quad W \sim \text{BM}([0, 10]). \quad (18)$$

We observe the position X_t at times $t = 1, 3, 5, 7$, and 9 with independent $\mathcal{N}(0, 0.09)$ observational noise. We set the true path to be the sine wave $X_t = \sin(4t)$, thereby providing an example of model misfit, where

the true path is not consistent with the Bayesian model. Lastly, we discretize W_t at 200 equally spaced times between $t = 0$ and $t = 10$ and we discretize the SDE using a standard Euler solver.

We observe in Figures 3 and 4 that the parameter α and the paths X_t are multimodal under the posterior distribution. Some posterior paths have a similar frequency to the true sine solution ($\alpha = 16$), while other paths have a frequency that is twice as fast or half as fast. This multimodality makes the MCMC sampling for this problem challenging.

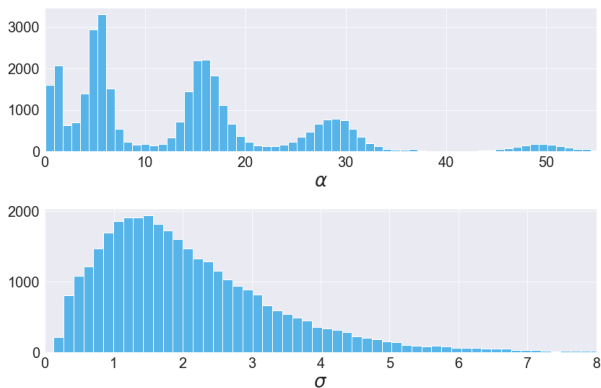


Fig. 3: Posterior pdf for α and σ parameters.

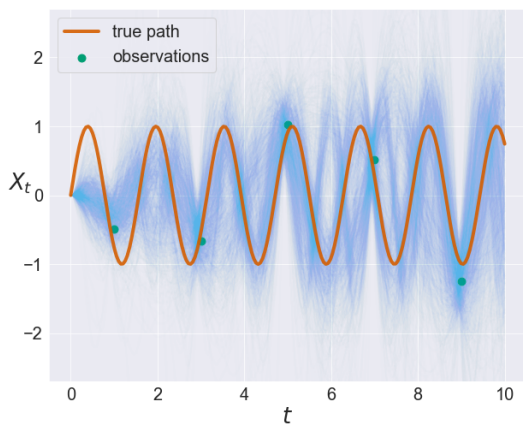


Fig. 4: Posterior paths exhibiting multimodality.

To infer the parameters α , σ , and W_t from the noisy observations, we compare five MCMC approaches:

1. A PCN-based sampler that simultaneously proposes PCN updates for W and Gaussian random walk up-

dates for (α, σ) with covariance matrix

$$\begin{pmatrix} 0.08 & 0.04 \\ 0.04 & 0.03 \end{pmatrix}. \quad (19)$$

2. The hybrid sampler developed in [18].
3. A modified FES sampler with $L = 8$ walkers and joint proposals that combine AIES and PCN moves to update all the parameters at once.
4. A modified FES sampler with $L = 100$ walkers and joint proposals.
5. A standard FES sampler with $L = 100$ walkers.

After pilot runs, we find that $M = 5$ is a near-optimal truncation parameter, and we fix this parameter for all the samplers (besides PCN).

We report the IATs for the various samplers in Table 3, and we show the ACF curves in Figure 5. These results demonstrate that using a large number of walkers improves the statistical efficiency when computing observables, a finding which is consistent with the past literature analyzing the performance of AIES. The minimum number of walkers that can be used in AIES is $M + 1$, where M is the dimension of the parameter space. However, it is recommended to use more walkers whenever possible. Foreman-Mackey and coauthors recommend using hundreds of walkers [10], and in some applications up to 2000 walkers have been used [1].

	Integrated autocorrelation times \div 1000				
	PCN	hybrid	joint, $L=8$	joint, $L=100$	$L=100$
α	51	38	23	11	12
σ	26	22	18	6.6	8.1
ϕ_1	5.7	1.5	6.3	1.0	1.6
ϕ_{10}	5.9	1.6	2.8	2.0	0.39
ϕ_{100}	5.8	1.2	2.5	1.8	0.30

Table 3: IATs for α , σ and several KL coefficients with the smallest IATs in bold. All IATs have been divided by 1000 to improve readability.

On the surface, it seems efficient to apply FES with a joint proposal that simultaneously updates the AIES subspace and the complementary subspace, since the joint proposal requires only half as many iterations to refresh a walker's position. However, Table 3 reveals that the joint proposal is less than twice as efficient as standard FES, because many of the joint parameter updates are rejected. With the joint proposal, the mixing is only 1.1-1.6 times faster within the AIES subspace, and the mixing is over five times slower in the complementary subspace. The advantages of the Metropolis-within-Gibbs strategy versus the joint update strategy depend on the particular statistics being calculated.

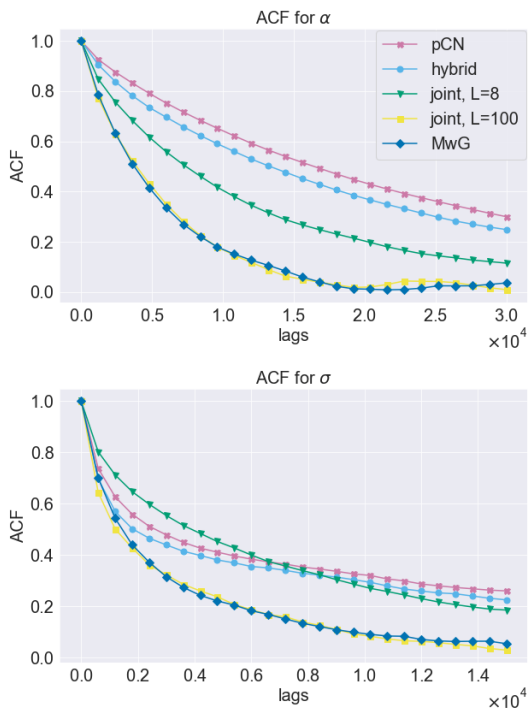


Fig. 5: ACF curves for α and σ parameters.

Lastly, we find that FES is a more efficient sampler compared to the hybrid sampler of [18]. FES has faster integrated autocorrelation times than the hybrid sampler for all observables. In addition, FES eliminates the major limitation of the hybrid sampler, which is the long adaptation period required for estimating the posterior covariance matrix. In Figure 6, we show the estimated variance for α and σ parameters using the hybrid sampler. More than one million iterations are needed for these variance estimates to stabilize. Because the hybrid sampler tunes its proposals based on the estimated posterior covariance matrix, the method does not obtain its full efficiency for over a million iterations. Since gradient-free functional samplers are often used with computationally intensive forward models, an adaptation period in the millions can be prohibitively expensive.

5 Conclusion

In this work, we introduced the functional ensemble sampler (FES). The FES requires no gradients, it is easy to code, and it is parallelizable. These factors help make FES a robust and widely applicable sampler for infinite-dimensional Bayesian inverse problems.

In two numerical examples, we demonstrated the benefits of using FES. First, we showed how FES can

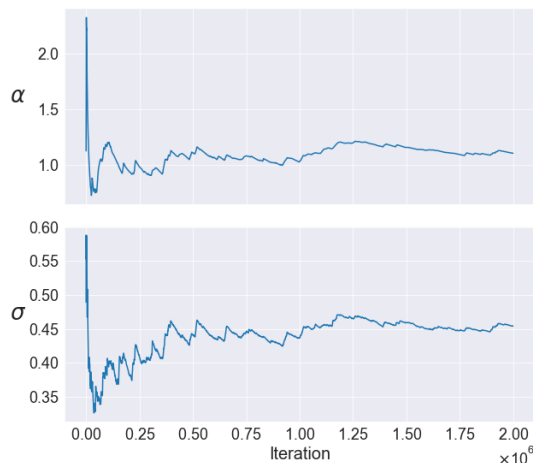


Fig. 6: Variance estimates for α and σ using the adaptive hybrid sampler.

improve the sampling speed of PCN by two orders of magnitude when parameters in the posterior distribution are correlated. Second, we showed how FES outperforms other gradient-free samplers when the posterior distribution is mildly multimodal.

We acknowledge two opportunities to improve the performance of FES further. First, new approaches could be developed to identify a likelihood-informed subspace where enhanced sampling is most essential. Second, after isolating a low-dimensional subspace for enhanced sampling, we find that AIES is typically an efficient sampler. However, other more efficient samplers might be available in the case of extreme multimodality, which is acknowledged in [11] to be the main limitation of AIES.

In conclusion, FES pushes the limits of the MCMC approach to solving infinite-dimensional inverse problems. Despite having a few limitations, the method offers a practical and powerful solution for many sampling problems where PCN fails, and we recommend FES as a general-purpose gradient-free sampler.

Acknowledgements We thank Christopher Nemeth, Gideon Simpson, and Jonathan Weare for useful conversations. JC was supported by EPSRC grant EP/S00159X/1. RJW was supported by the National Science Foundation award DMS-1646339 and by New York University’s Dean’s Dissertation Fellowship. The High End Computing facility at Lancaster University provided computing resources.

References

1. Akeret, J., Seehars, S., Amara, A., Refregier, A., Csilaghy, A.: Cosmohammer: Cosmological parameter esti-

- mation with the MCMC hammer. *Astronomy and Computing* **2**, 27–39 (2013)
2. Beskos, A., Girolami, M., Lan, S., Farrell, P.E., Stuart, A.M.: Geometric MCMC for infinite-dimensional inverse problems. *Journal of Computational Physics* **335**, 327–351 (2017)
 3. Beskos, A., Jasra, A., Law, K., Marzouk, Y., Zhou, Y.: Multilevel sequential Monte Carlo with dimension-independent likelihood-informed proposals. *SIAM/ASA Journal on Uncertainty Quantification* **6**(2), 762–786 (2018)
 4. Beskos, A., Roberts, G., Stuart, A., Voss, J.: MCMC methods for diffusion bridges. *Stochastics and Dynamics* **8**(03), 319–350 (2008)
 5. Cotter, S.L., Roberts, G.O., Stuart, A.M., White, D.: MCMC methods for functions: Modifying old algorithms to make them faster. *Statistical Science* pp. 424–446 (2013)
 6. Coullon, J., Pokern, Y.: Mcmc for a hyperbolic bayesian inverse problem in traffic flow modelling. arXiv preprint arXiv:2001.02013 (2020)
 7. Cui, T., Law, K.J., Marzouk, Y.M.: Dimension-independent likelihood-informed MCMC. *Journal of Computational Physics* **304**, 109–137 (2016)
 8. Cui, T., Martin, J., Marzouk, Y.M., Solonen, A., Spantini, A.: Likelihood-informed dimension reduction for nonlinear inverse problems. *Inverse Problems* **30**(11), 114,015 (2014)
 9. Dunlop, M.M., Stuart, A.M.: The Bayesian formulation of EIT: Analysis and algorithms. *Inverse Problems and Imaging* **10**(4), 1007–1036 (2016)
 10. Foreman-Mackey, D., Hogg, D.W., Lang, D., Goodman, J.: emcee: the MCMC hammer. *Publications of the Astronomical Society of the Pacific* **125**(925), 306 (2013)
 11. Goodman, J., Weare, J.: Ensemble samplers with affine invariance. *Communications in Applied Mathematics and Computational Science* **5**(1), 65–80 (2010)
 12. Iglesias, M.A., Lin, K., Stuart, A.M.: Well-posed bayesian geometric inverse problems arising in subsurface flow. *Inverse Problems* **30**(11), 114,001 (2014). DOI 10.1088/0266-5611/30/11/114001. URL <https://doi.org/10.1088/0266-5611/30/11/114001>
 13. Metropolis, N., Rosenbluth, A.W., Rosenbluth, M.N., Teller, A.H., Teller, E.: Equation of state calculations by fast computing machines. *Journal of Chemical Physics* **21**(6), 1087–1092 (1953)
 14. Roberts, G.O., Rosenthal, J.S.: Examples of adaptive MCMC. *Journal of Computational and Graphical Statistics* **18**(2), 349–367 (2009)
 15. Rudolf, D., Sprungk, B.: On a generalization of the preconditioned Crank–Nicolson Metropolis algorithm. *Foundations of Computational Mathematics* **18**(2), 309–343 (2018)
 16. Sokal, A.: Monte Carlo methods in statistical mechanics: Foundations and new algorithms. In: *Functional integration*, pp. 131–192. Springer (1997)
 17. Stuart, A.M.: Inverse problems: a Bayesian perspective. *Acta Numerica* **19**, 451 (2010)
 18. Zhou, Q., Hu, Z., Yao, Z., Li, J.: A hybrid adaptive MCMC algorithm in function spaces. *SIAM/ASA Journal on Uncertainty Quantification* **5**(1), 621–639 (2017)